J-PARC RCS NON-LINEAR FREQUENCY SWEEP ANALYSIS

A. Schnase*, S. Anami, E. Ezura, K. Haga, K. Hara, K. Hasegawa, M. Nomura, C. Ohmori, A. Takagi, F. Tamura, M. Toda, M. Yamamoto, M. Yoshii, KEK&JAEA/J-PARC, Tokai-Mura, Ibaraki-Ken, 319-1195 Japan

Abstract

A standard method to measure the S_{21}-transfer function of a system of amplifier and cavity is using a network analyzer (NWA) and a linear frequency sweep.

However, to characterize the transfer function of the broadband (Q=2) RCS (Rapid Cycling Synchrotron) RF system, we want to analyze several harmonics at same time under high power ramping conditions. A pattern driven DDS system simulates accelerator operation. During the 20ms acceleration part of the RCS cycle, an oscilloscope with large memory, triggered by ramp-start captures the RF-signals. The data are analyzed offline with a process like down-conversion in a multi-harmonic LLRF-system, giving multi-harmonic amplitude and phase information. With this setup in the test phase we were able to cure resonances in the RF systems before installation to the tunnel.

RCS is in the commissioning phase and has reached the milestone of acceleration to final energy and extraction of the 3GeV beam. 10 RF systems are in operation, and the low-level RF system controls the fundamental (h=2) and the second harmonic (h=4). The multi-harmonic analysis helps checking the behavior of the high power part of the RF system also at other harmonics.

INTRODUCTION

Acceleration to 1-MW beam power in the J-PARC RCS with given ring circumference is only accomplishable by using high-field gradient magnetic alloy (MA) cavities [1]. The optimum cavity quality factor for RCS is approximately Q=2. Introducing a parallel inductor [2], the Q-value of the cavities loaded with uncut cores is changed from 0.6 to 2.0.

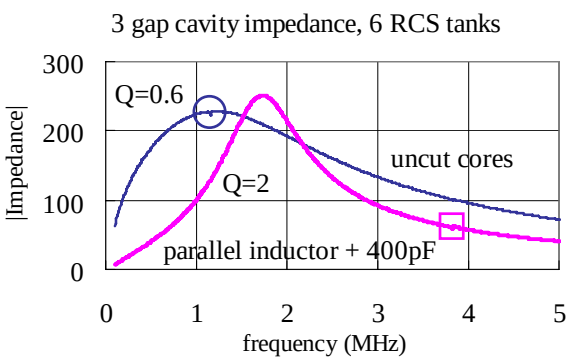

Figure 1: Cavity impedance (3 gaps in parallel) with and without parallel inductor before removal of resonances.

The cavity impedance with push-pull tube amplifier connected is shown for both cases with / without parallel inductor in Figure 1. The measurement with uncut cores only (blue curve) shows a small dent near 1.15 MHz, marked by a circle. The measurement with additional parallel inductor (pink curve) shows a small discontinuity near 3.8 MHz (later 3.9 MHz with different MA cores), marked by a square. In the following, the set-up to investigate is described.

SIMULATION OF 25HZ OPERATION

The circuit in figure 2 provided the low-level RF signal for 25 Hz long-run tests [3, 4] to the test-bench located in the Hendel building. Frequency and amplitude pattern (Fig. 3) for the 40 ms period are defined with 40000 points at 1MHz sample rate and send to the digital synthesizer. This system is independent from the digital LLRF system [5] for RCS operation with up to 12 cavities, which was prepared for installing into RCS at this time.

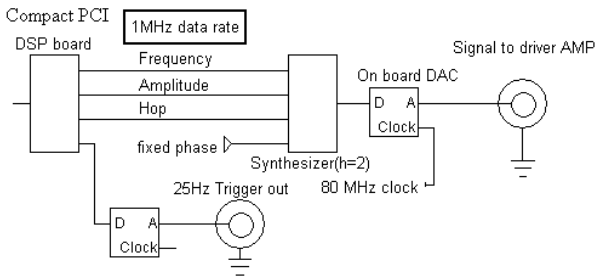

Figure 2: The low-level synthesizer for 25 Hz tests.

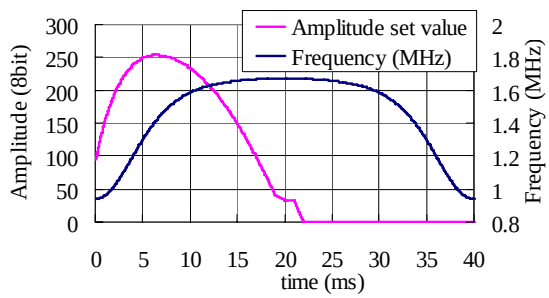

Figure 3: 25 Hz amplitude and frequency (h=2) pattern.

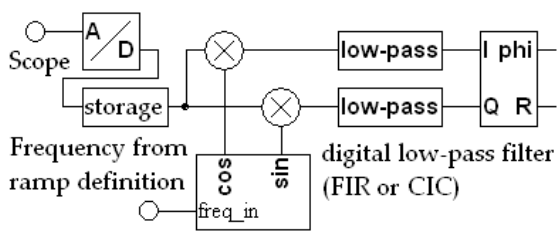

Figure 4: Offline data processing like an IQ-receiver.

Tube amplifier signals: control grid, screen grid, anode, and cavity gap monitor were sampled with 25 MSPS, so

that the 20 ms acceleration part of the ramp is captured with 500000 points. The data were processed offline (figure 4) for the harmonics (h=2, 4, 6) in a similar way to IQ-down-conversion in the LLRF system [5].

FINDING RESONANCES

The circle in figure 1 refers to a resonance near 1.15 MHz, which we traced to the filter between anode and anode power supply. This resonance was cured by a serial damper circuit of 5 Ohm + 24nF in parallel to the existing 8nF filter capacitor in each amplifier (figure 5). With two 10 Ω, 50 W resistors in parallel, a temperature up to 150 deg was measured in a long run test. Therefore, finally 6 parallel 30 Ω resistors (50 W) are used (fig. 6). This damper was installed to all 10 RCS tube amplifiers.

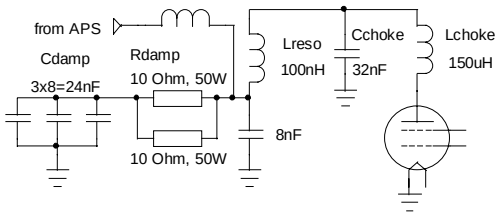

Figure 5: Simplified schematic of damper circuit

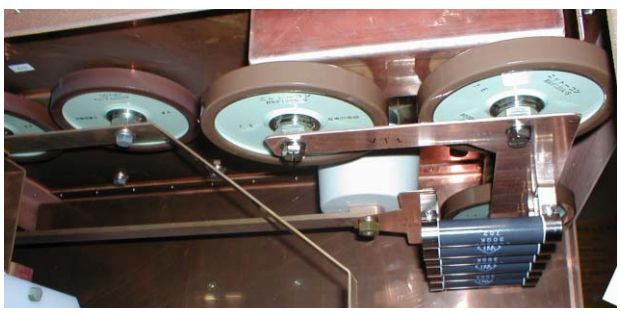

Figure 6: The damper circuit on one amplifier side: 3x8nF high voltage capacitors and 6x30 Ohm load resistors.

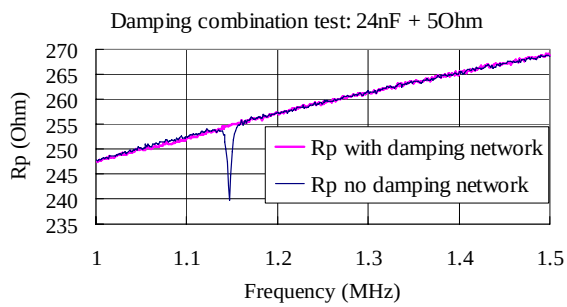

Figure 7: The resonance near 1.15 MHz in R_p measured by network analyzer disappears with the damper circuit.

Figure 7 shows that the resonance at 1.15 MHz is damped. This is confirmed by the screen grid current monitor signals of both tubes in figure 8. The small dip on the left (8a)) near 3.6 ms, equivalent to a frequency of 1.15 MHz (from figure 3) disappears with the damper, as seen on the right (8b)). The next resonance at 5.2 ms corresponds to 1.3 MHz of the driving frequency at (h=2). The NWA did not see this resonance (fig. 7) at the cavity.

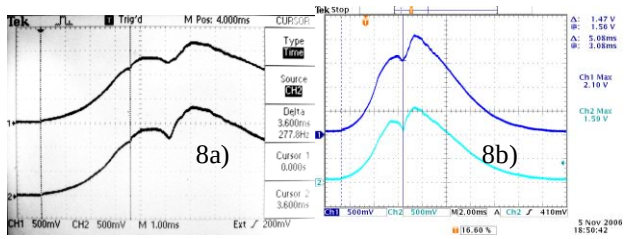

Figure 8a) The screen grid current indicates a resonance at 3.6 ms without damper. 8b) With damper the resonance disappears. The next resonance near 5.2ms remains.

Mica Capacitors from Cathode to Ground

Figure 9 gives a schematic of the distribution of 750nF Mica capacitors at the tube socket. One of the capacitors was taken out and measured. Figure 10 shows that such a capacitor has a first resonance at 2.6 MHz and multiple resonances at higher frequencies.

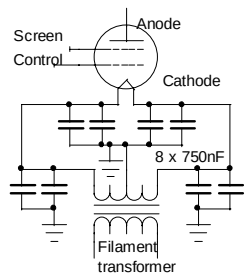

Figure 9: 750 nF MICA capacitors at tube socket

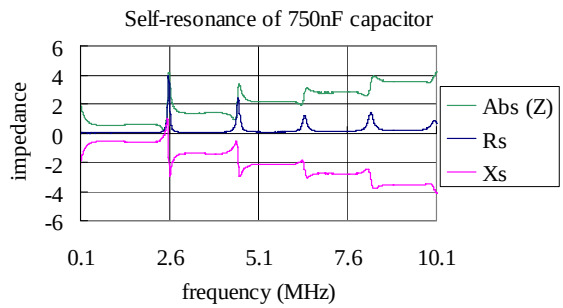

Figure 10: 2.6 MHz resonance of 750 nF MICA cap

The multi-harmonic analysis during high power test revealed the cause of the resonance in figure 8. Near 5ms in the cycle, the fundamental (h=2) is 1.3 MHz. Then the 2nd harmonic (h=4) is 2.6 MHz. The purple line in figure 11 shows a dip at (h=4) of the anode voltage.

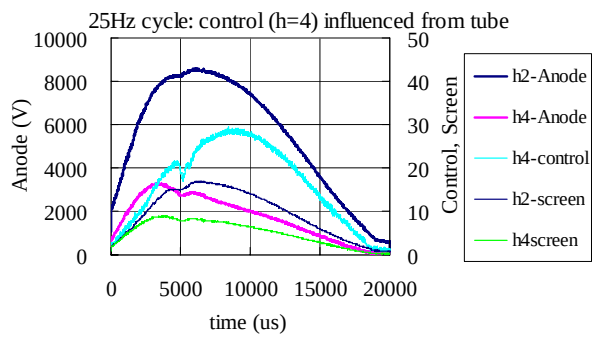

Figure 11: High power test shows a 2.6 MHz resonance.

The cathode current is almost same as the anode current and the RF component including (h=4) goes through the MICA capacitors. Then the (h=4) resonance appears on the control grid with respect to ground. This resonance could not be seen with NWA at the gap, because with NWA, the tubes are off, and there is no RF cathode current through the MICA capacitors, which act like resonators. The issue was solved by a serial damper combination of a 200nF MICA capacitor and 0.33 Ohm in parallel to each of the four 750 nF MICA capacitors near to the tube socket in all RCS amplifiers.

DC-Blocking Capacitor

The square in figure 1 marks a resonance near 3.9 MHz. We proved that this is not related to the external inductor [2], but to the arrangement of 16x 8 nF capacitors used as DC block between each anode and cavity (Fig. 12). The copper tape (arrow) is an additional connection of copper slabs on same potential. It reduces the inductance and shifts the resonance to frequencies higher than the (h=6) range of RCS. Figure 12 (left) confirms that the resonance near 3.9 MHz, the 3rd harmonic of the (h=2) stimulus at 1.3 MHz, disappears when the copper tape is applied.

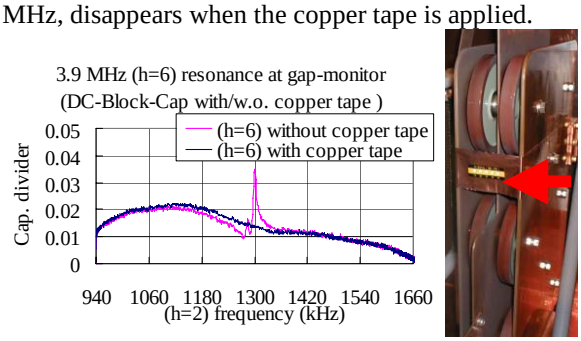

Figure 12: Left: 3.9 MHz (h=6) resonance at cavity gap monitor. Right: 128nF DC blocking capacitor. The arrow marks the additional copper slab connection.

Parasitic Resonance

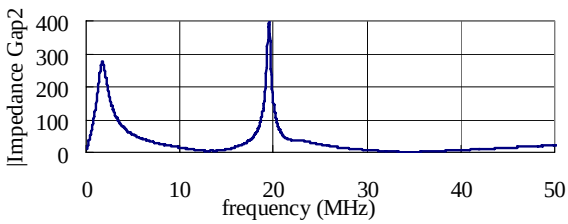

Figure 13: Parasitic cavity resonance near 20 MHz

The parasitic resonance near 20 MHz in fig. 13 is related to the busbars that connect 3 gaps in parallel to the tube amplifier. So far we could not measure any negative effect on the beam. With another RCS cavity for testing at the Hendel test site, we continue to study suitable damping methods independent of RCS operation.

Harmonic Content in RCS Operation

2 Million points captured at 100MSPS rate for each of the 10 RCS cavities were analyzed according to fig. 4. Figure 14a shows the ratio of the 2nd harmonic A_4 to the fundamental A_2 for selected RCS cavities. We see the expected reduction of A_4 due to push-pull operation of the tube amplifiers. The remaining A_4/A_2 content is smallest at cavity 2 and highest at cavity 3. After circa 6 ms, the 2nd harmonic content is less than 2% for all 10 cavities. Figure 14b shows the ratio of the 3rd harmonic A_6 to A_2. The peak near 1ms corresponds to 0.96 MHz for A_2. The highest 3rd harmonic content is 11% at cavity 7. The next harmonic A_8/A_2 is smaller than 0.5% for all 10 cavities. This data demonstrates that the resonances have been cured effectively. But we have to consider the harmonic content when we measure the synchrotron frequency [6].

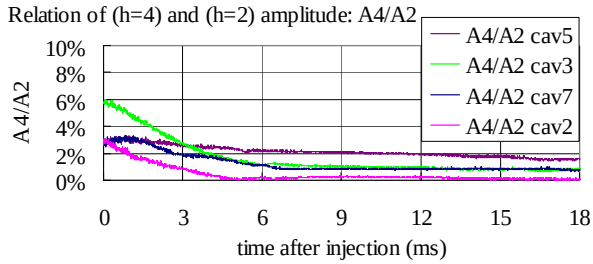

Figure 14a: 2nd Harmonic content at cavities 2, 3, 5, and 7. The data are arranged by A_4/A_2 at 18ms.

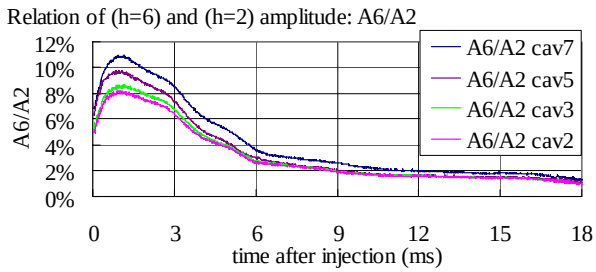

Figure 14b: 3rd Harmonic content at cavities 2, 3, 5, and 7.

SUMMARY

We removed 3 resonances in the RF systems so that the RCS operating range from 0.938 MHz (h=2; 181 MeV) to 5.1 MHz (h=6; 3 GeV) is free of unwanted resonances. Further studies will tackle the parasitic resonance.

REFERENCES

[1] C. Ohmori et. al, “Possible upgrade scenario for J-PARC ring RF”, EPAC 08, MOPP104

[2] A. Schnase et. al. “MA cavities for J-PARC with controlled Q-value by external inductor”, PAC07, p. 2131ff

[3] M. Yamamoto et. al, “High Power Test of MA Cavity for J-PARC RCS”, PAC07, p. 1532-1534

[4] M. Yoshii et. al, “J-PARC Ring RF Accelerating Systems”, PAC07, p. 1511-1513

[5] F. Tamura et. al, “Low Level RF Control System of J-PARC Synchrotrons”, PAC 2005, p3624, Knoxville

[6] F. Tamura et. al, “Beam acceleration with full-digital LLRF control system in the J-PARC RCS”, EPAC 08.